Quantum Cellular Automaton Device Using the Image Charge Effect

1998 Jpn. J. Appl. Phys. 37 2433

(http://iopscience.iop.org/1347-4065/37/5R/2433)

Jpn. J. Appl. Phys. Vol. 37 (1998) pp. 2433–2438
Part 1, No. 5A, May 1998

Quantum Cellular Automaton Device Using the Image Charge Effect

Nan-Jian WU, Naoto SHIBATA[1] and Yoshihito AMEMIYA

Department of Electrical Engineering, Faculty of Engineering Hokkaido University, Sapporo 060-8628, Japan
[1]*Dai Nippon Printing Co., Ltd. Tokyo 141-0031, Japan*

(Received November 25, 1997; accepted for publication February 16, 1998)

A quantum cellular automaton (QCA) device that uses the image charge effect is proposed. This image-charge QCA device is constructed from many unit cells on a metal substrate covered with an insulator layer. Each unit cell consists of four quantum dots and two excess electrons. Two positive image charges in the metal substrate maintain the charge neutrality of each cell. The distance between two neighboring cells is designed to allow intercellular electron tunneling. The image-charge QCA cell can overcome two basic problems: establishing charge neutrality in each cell and loading electrons easily and precisely. We designed signal-transmission and elemental logic gate circuits using these image-charge QCA cells, and simulated operation of the circuits by computer simulation. It is demonstrated that the image-charge QCA circuits can perform signal transmission and elemental logic operations and that electrons (two per cell) can be easily loaded into the image-charge QCA circuits.

KEYWORDS: quantum, cellular automaton, QCA, image charge, device

1. Introduction

One of the challenges in microelectronics is the development of next-generation LSIs based on new paradigms for information processing. The quantum cellular automaton (QCA)[1–3] is a promising architecture for such LSIs because it affords the possibility of producing data-processing systems with a compact construction. To materialize the QCA systems, we must devise a feasible device structure for QCAs. This paper proposes such a device structure, namely, *a quantum cellular automaton device that uses the image charge effect.*

The QCA is a data-processing system consisting of a two-dimensional arrangement of coupled unit cells. Each unit cell consists of diagonally-positioned quantum dots, two of which are occupied by excess single electrons. A unit cell has two polarization states, which can be used to decode the binary information "1" and "0". The layout of the QCA circuit is designed so that the ground state of the electron configuration under a given input is equivalent to the result of the computation. By arranging the unit cells in an appropriate layout, elemental logic gate circuits, such as AND and OR gates, can be constructed.

To develop the QCA for use in actual devices, two basic problems must be solved: that is, 1) how to establish the charge neutrality in each cell, and 2) how to load exactly two electrons into each cell. These two problems will be explained in detail.

The first problem is the establishment of charge neutrality in the unit cell. The QCA is a device that uses an intercellular interaction between the unit cells. To make the QCA perform logic operations correctly, the intercellular interaction must be a short-range interaction—that is, an interaction that works only between the nearest-neighbor unit cells and does not work between the separated unit cells. In the QCA, the intercellular interaction is generated by dipoles of the cell charge distribution. Hence, each cell must have a neutral charge so that the intercellular interaction can be regarded as a local interaction.[1)] The second problem is the loading of electrons. To make the QCA circuit work correctly, two and only two electrons must be loaded into each cell. A possible physical means of achieving charge neutrality and loading electrons is to implant exactly two donor impurity atoms into the center of each cell. The two impurity atoms supply two electrons and two positive ions into each cell. The two electrons can move among the dots in the cell and the positive ions can maintain the charge neutrality in the cell. However, such impurity implantation into a designated position requires nanometer-order precision, so it is not practical for use in LSI fabrication.

We propose a feasible device structure for overcoming the above problems. The device structure uses the image-charge effect to maintain charge neutrality in each cell. Impurity implantation is unnecessary. Furthermore, intercellular tunneling is allowed and is used to load the two electrons into each cell. We call this device an *image-charge QCA*. In the following sections we first present the structure of the image-charge QCA and describe its operation (§2). We then present designs of several circuit elements, i.e., a signal-transmission wire and logic gates, using the image-charge QCA cells and analyze the operations of the designed image-charge QCA circuits by computer simulation. We will demonstrate that the image-charge QCA circuits can perform signal transmission and elemental logic operations (§3). We will then describe the simulation of electron loading into each cell and will show that electron loading can be easily performed by injecting electrons from one end cell into the cell circuit, two electrons per cell (§4). We also discuss the writing and reading operations (§5). Finally, we will summarize the main results (§6).

2. Image-Charge QCA Unit Cell

Figure 1(a) shows the schematic structure of the image-charge QCA circuit. The circuit is constructed from many unit cells on a metal (or conductive) substrate covered with an insulator layer. The distance between two neighboring cells is designed to allow intercellular electron tunneling so that electrons can move among all the cells in the image-charge QCA circuit. Figure 1(b) depicts the image-charge QCA unit cell and its two polarization states. The unit cell consists of four quantum dots and two electrons. The cell is designed such that the electrons can tunnel among the dots. When two excess electrons are injected into the unit cell, two corresponding image charges originate in the metal substrate. The two positive-image charges maintain the charge neutrality of each cell. A dipole is formed out of the paired electron and image charge. We hereafter use the symbol shown in Fig. 1(c) to

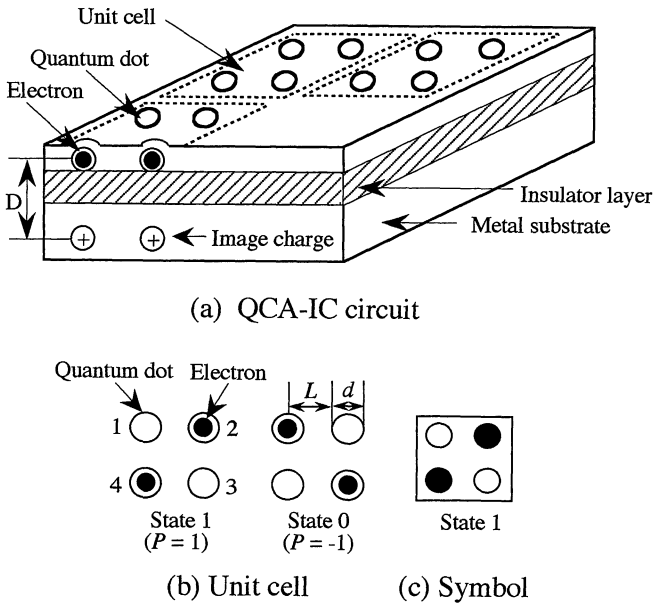

Fig. 1. (a) Schematic structure of an image-charge QCA circuit; (b) unit cell and two states of polarization; (c) cell notation.

represent an image-charge QCA unit cell.

The polarization of the excess electrons in the cell is defined as

$$P = \frac{(\rho_2 + \rho_4) - (\rho_1 + \rho_3)}{\rho_1 + \rho_2 + \rho_3 + \rho_4}, \tag{1}$$

where ρ_i is the density of electrons on the i-th quantum dot [see Fig. 1(b)]. When two electrons occupy quantum dots 1 and 3, the polarization is $P = -1$, and when the two electrons occupy quantum dots 2 and 4, the polarization is $P = +1$. The polarizations "1" and "-1" can be used to decode binary values "1" and "0".

An image-charge QCA has two advantages when compared with the QCA. First, the charge neutrality in each cell can be maintained naturally by the image charge effect. Because positive image charges will originate in the metal substrate, corresponding to the excess electrons in the quantum dot [Fig. 1(a)], the charges of these electrons can be neutralized naturally by the positive image charges. Second, because intercellular electron tunneling is allowed, electron loading can be easily performed by injecting electrons from one end cell into the cell circuit at the rate of two electrons per cell. Consequently, the image-charge QCA circuit can be fabricated using existing technologies. For example, it is possible to fabricate an image-charge QCA cell if we use pattern-dependent oxidation on a SIMOX substrate[4] and the nano-oxidation process.[5]

3. Operation of Image-Charge QCA Circuits

We simulated the operation of the QCA circuits by the method described below. In describing this process, we will first determine the ground state of the QCA circuit under given inputs. Then, we will confirm that the corresponding outputs are the correct results of the computation.

3.1 Image-charge QCA model

We used an extended Hubbard-type Hamiltonian[1] to describe the image-charge QCA circuit:

$$\begin{aligned} H = & \sum_{m,i,\sigma} E_0 n_{mi\sigma} + \sum_{m,i\neq j,\sigma} t_{mi,mj} c^+_{mi\sigma} c_{mj\sigma} \\ & + \sum_{m\neq k,i,j,\sigma} t_{mi,kj} c^+_{mi\sigma} c_{kj\sigma} \\ & + \frac{1}{2} \sum_{m,i,\sigma} U_{mi,mi} n_{mi\sigma} n_{mi-\sigma} \\ & + \frac{1}{2} \sum_{m,i\neq j,\sigma,\sigma'} U_{mi,mj} n_{mi\sigma} n_{mj\sigma'} \\ & + \frac{1}{2} \sum_{m\neq k,i,j,\sigma,\sigma'} U_{mi,kj} n_{mi\sigma} n_{kj\sigma'} \end{aligned} \tag{2}$$

Here, m and k denote the cells in the circuit, and i and j denote quantum dot i in cell m and dot j in cell k. The notation $c^+_{mi\sigma}$ ($c_{mi\sigma}$) is the creation (annihilation) operator for an electron with spin σ at site i in cell m, and $n_{mi\sigma}$ is the number operator of the electron with spin σ at site i in cell m. The notation $t_{mi,kj}$ is the overlap integral, which represents the interdot coupling between the two quantum dots i in cell m and j in cell k, and E_0 is the on-site energy for the i-th dot. $U_{mi,kj}$ is the Coulomb potential energy between two excess electrons located at dot i in cell m and dot j in cell k:

$$U_{mi,kj} = \frac{2q^2}{4\pi\varepsilon_0\varepsilon_r} \left[\frac{1}{|\boldsymbol{R}_{mi} - \boldsymbol{R}_{kj}|} - \frac{1}{\sqrt{|\boldsymbol{R}_{mi} - \boldsymbol{R}_{kj}|^2 + D^2|}} \right], \tag{3}$$

where $\boldsymbol{R}_{mi}$ and $\boldsymbol{R}_{kj}$ are positions of dot i in cell m and dot j in cell k and D is the distance between the excess electron and the corresponding image charge. $U_{mi,mi}$ is the charging energy for a single dot, which can be obtained by replacing $\boldsymbol{R}_{mi} - \boldsymbol{R}_{kj}$ with $d/3$ (d: the diameter of the quantum dot).

3.2 Simulation method

We used the Monte-Carlo simulation method, described in ref. 6, to calculate the electron configuration for the lowest free energy at a given physical temperature T. During simulation an iteration parameter, a virtual temperature T_v, was introduced (T_v is different from the physical temperature T). Initially, we selected a current electron configuration randomly and started a "trial" at a sufficiently high virtual temperature $T_{\mathrm{v}0}$. The trial consists of the following steps: 1) changing the current electron configuration into a new configuration by making a unitary transformation, 2) calculating the energy difference between the two configurations, and 3) deciding to adopt the new configuration using the Metropolis algorithm. We then continued the trial while exponentially lowering T_v at a gradual rate. When the virtual temperature is lowered to a sufficiently low value, the ground state of the electron configuration for the given physical temperature T and given inputs can be obtained.

This simulation method has some advantages, compared with the intercellular Hartree approximation.[2] First, it allows calculation of the ground state of a many-body system without dependence on the choice of the initial state. Second, it can be used to calculate the ground state of the entire image-charge QCA circuit by including the exchange and correlation effects between the cells. Third, this method is applicable to the simulation of an image-charge QCA circuit operation at

any physical temperature.

3.3 Signal transmission

We designed signal-transmission circuits, such as linear, angled, and fan-out arrays, using the image-charge QCA cells. We calculated the ground state of the electron configurations in each circuit for a given input, assuming the physical temperature 0 K. We confirmed that the ground state corresponds to the electron configuration in which the output is 1 (0) for the input of 1 (0); that is, the signal can be accurately transmitted along the signal-transmission arrays. The values of the image-charge QCA circuit parameters are as follows. We took the diameter d of the circular quantum dot to be 10 nm. The distance L between the centers of the two nearest-neighbor dots in the unit cell was taken to be 20 nm. The distance F between the centers of the nearest-neighboring cells was 42 nm. The distance D between the excess electron and the image charge was taken to be 20 nm. The dielectric constant ε_r was taken to be 10. The magnitude of the transfer integrals between the quantum dots in cell m was set to t_{m1m2}=t_{m2m3}=t_{m3m4}=t_{m1m4}=0.03 meV and t_{m1m3}=t_{m2m4}=0 (m = 1, 2, 3,...). The magnitude of the transfer integrals between nearest-neighbor dots i and j in neighbor cells m and k was set to t_{mikj} = 0.003 meV. The tunneling between the input cell(s) and the other cells is forbidden (t = 0). For simplicity, E_0 was considered to be 0. The simulated results are described below. Figure 2(b) shows the typical development of the free energy of a five-cell linear array circuit for an input "1" with the number t of the Monte Carlo trials. After repeated trials, the free energy decreased and reached a stable state, that is, the ground state. The ground states, as shown in Fig. 2(a), correspond to the condition in which signal 1 (P = +1) is accurately transmitted from one end to the other. During the calculation process, the virtual temperature T_v decreased exponentially, $T_v = 4\exp(-10^{-6}t)$, where t is the number of Monte Carlo trials.

Figure 3 gives the calculated results of the ground state configuration for the angled array and fan-out array circuits. Figure 3(a) shows the ground state of the five-cell angled array circuits for an input of "1". The result shows that the input binary signal 0 or 1 (P = +1 or −1) can be accurately transmitted from one end to the other through the circuit. Figure 3(b) shows the ground state of the fan-out array circuit, which consisted of seven unit cells for an input of "1". The input signal fanned out correctly to drive two output ends.

3.4 Logic gates

Figure 4 shows the ground states of the electron configurations in the image-charge QCA elemental logic gate circuits: (a) an inverter gate and (b) a majority logic gate. The inverter gate consisted of six unit cells. The stable electron configuration for an input of "1" is illustrated in Fig. 4(a). The result shows that the polarization P of the output cell changed in inverse relation to that of the input cell; if the polarization of the input cell was 1, then the polarization of the output cell was −1, and if the input was −1, then the output was 1. Thus, the ground state corresponded to a correct inverter operation.

Figure 4(b) illustrates the simulated result of the majority logic gate, which consisted of five cells (three input cells, a central cell, and an output cell). It can be seen from the stable

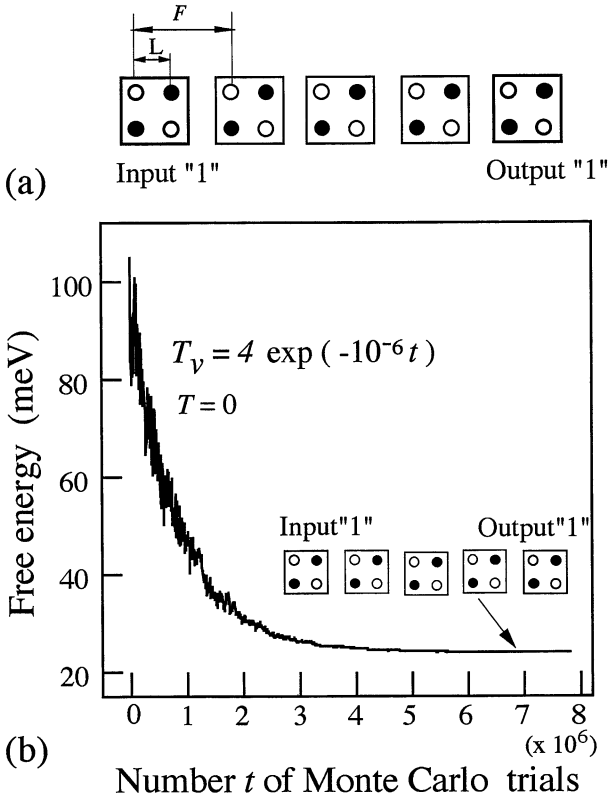

Fig. 2. Operation of a linear array circuit: (a) a five-cell linear array circuit; (b) typical development of the free energy of the array circuit plotted against the number t of Monte Carlo trials.

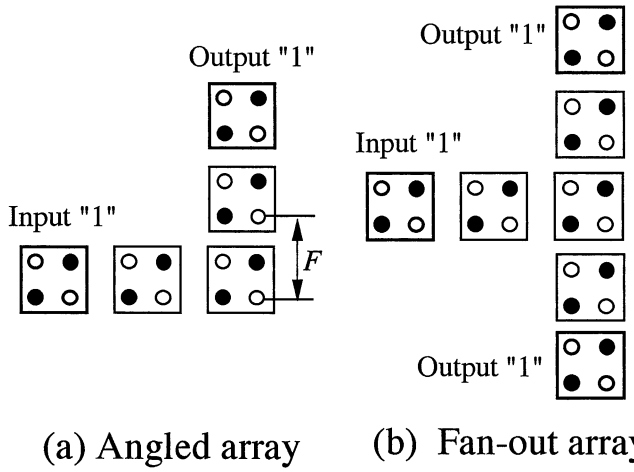

Fig. 3. Operations of signal-transmission array circuits: (a) angled array circuit for an input of "1", (b) fan-out array circuit for an input of "1".

electron configurations that the output cell of the gate always lined up so as to match the majority of the input cells.

3.5 Operation at various temperatures

We also calculated the stable-state electron configuration in the image-charge QCA circuit at non-zero temperatures. Figure 5 gives the simulation result for a five-cell linear array circuit with an input of "0". At high temperatures, an electron will extend over all the quantum dots, hence, a binary state cannot be defined. For temperatures below 10 K, the cell can distinctly represent a 1-0 signal; the signal 0 (P = −1) was accurately transmitted from one end to the other through the

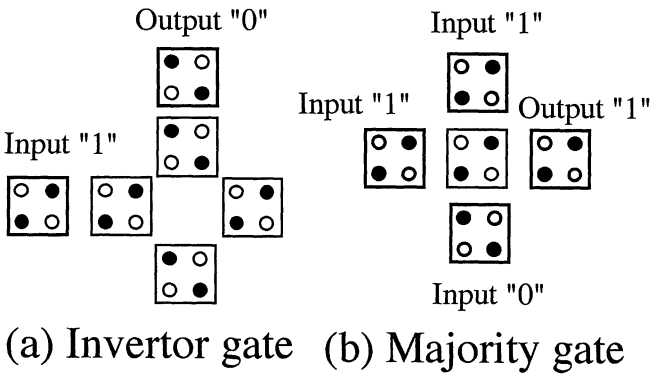

Fig. 4. Operations of logic gate circuits: (a) invertor circuit for an input of "1"; (b) majority logic circuit for two inputs of "1" and one input of "0".

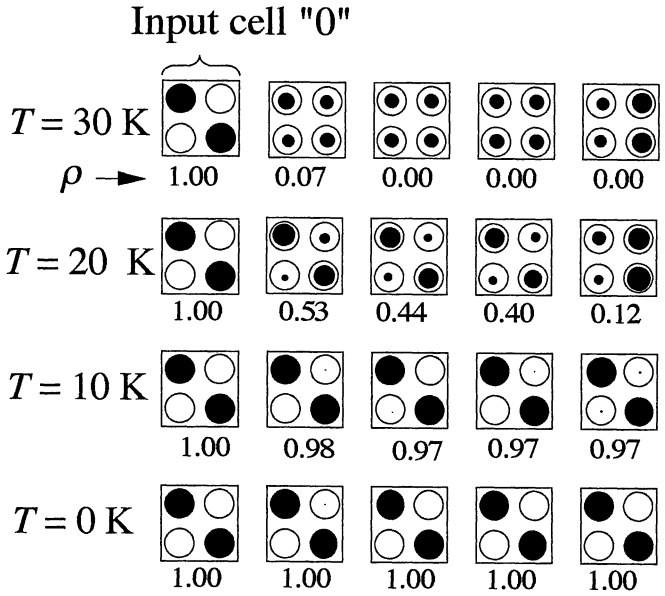

Fig. 5. Operations of a five-cell linear array circuit at various temperatures. The diameter of the solid dots indicates the charge density at each dot, and the values below each cell indicate the polarization in the cell. The distance F between the centers of the nearest-neighboring cells is 46 nm.

circuit. If we consider scaling down the size of the image-charge QCA cell, the operating temperature will increase.

3.6 Optimum range of parameters

We investigated the range of the dimension parameters that produce the correct electron configuration at the ground state. We analyzed the linear array, the inverter, and the majority gate. We changed the distance D between the electron and the image charge and the distance F between the centers of the nearest-neighbor cells while calculating the operations of the majority logic gate circuit. Figure 6 shows the optimum range of the parameters D and F for the majority logic gate in Fig. 4(b). If these parameters are designed to be within the optimum range, the circuit can perform correctly and the absolute value of the polarization of the input and output cells in the circuits will be larger than 0.9. In practice, an image-charge QCA circuit having parameters in the optimum range can be achieved using existing technologies. For other image-charge QCA circuits, a range similar to that of the majority logic gate can be obtained.

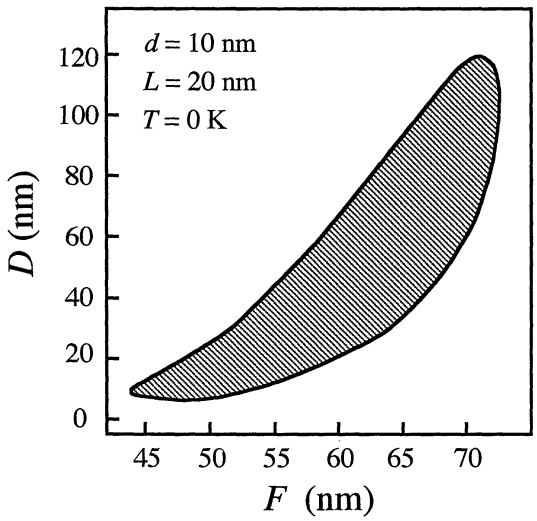

Fig. 6. Optimum range of the parameters D and F of a cell structure in the majority logic circuits.

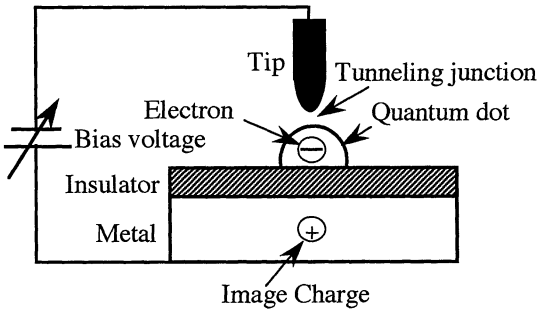

Fig. 7. Schematic of an electron injection system into a specific quantum dot using a STM/AFM tip.

4. Electron Loading

Here we consider the loading of electrons (two electrons on each cell). The method that we propose is as follows: 1) the electron is injected into a specific quantum dot and 2) electrons are dispersed into each cell. Figure 7 is a schematic representation of electron injection into a quantum dot by means of a scanning tunneling microscope (STM) [or atomic force microscope (AFM)] tip. The advantages of this method are the following. First, the injection method can be performed using existing techniques. Second, due to the Coulomb Blockade effect, the expected number of single electrons can be controlled by adjusting the bias voltage.[7] We calculated the operation of the STM/AFM electron injection using the Monte Carlo method.[8,9] Figure 8 shows the equivalent circuit of the injection system and the simulated dependence of the electron number in the quantum dot on the bias voltage at room temperature. When the bias voltage was set between 0.063 and 0.096 V, one electron tunneled into the quantum dot through the tunneling junction and occupied the dot in a stable configuration. When the bias was set between 0.145 and 0.19 V, two electrons tunneled into the quantum dot and occupied the dot stably. If the voltage is set to another value, the electron does not occupy the quantum dot stably. This result demonstrates that the desired number of single electrons

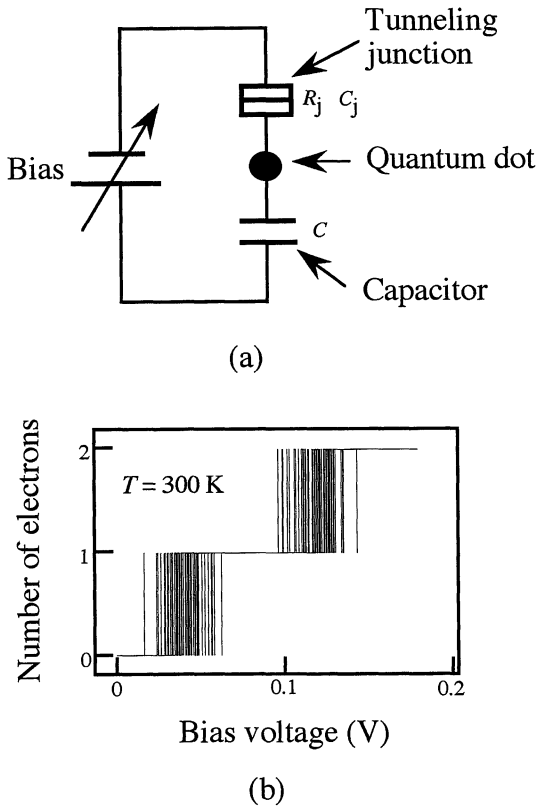

Fig. 8. (a) Equivalent circuit of an injection system ($C_j = 1$ aF; $R_j = 100$ MW; $C = 1$ aF); (b) simulated results of single-electron loading at room temperature.

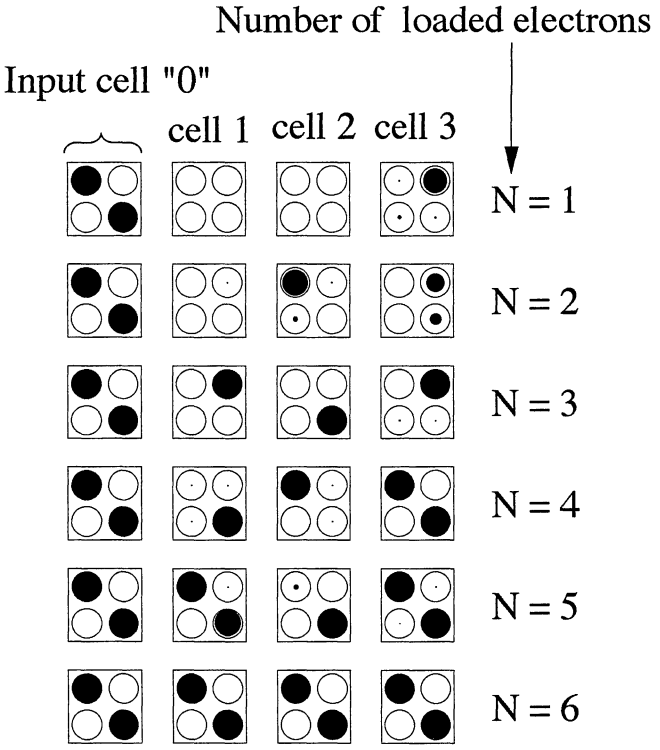

Fig. 9. Behavior of excess electrons in a four-cell linear array when various numbers of electrons are injected into the array.

can be loaded into a specific quantum dot by appropriately adjusting the bias voltage.

After injection into a specific dot, the electrons will tunnel among the cells to spread into the image-charge QCA circuit and will reach a stable configuration that has the lowest free energy. We simulated this process for a four-cell linear array. Figure 9 shows the simulation result for electron loading in a four-cell array, in which the input cell contains two electrons and the polarization of the input cell is fixed at 0. In this simulation, the electrons were loaded one by one at the upper-left quantum dot of cell 1. The ground-state electron configuration is shown in Fig. 9 for each number N of injected electrons. After six electrons (two electrons per cell) were loaded into the array, each cell kept two excess electrons and showed the same polarization as that of the input cell. This demonstrates that the electron loading can be easily performed by injecting electrons from one end cell into the image-charge circuit, two electrons per cell.

5. Writing and Reading Operations

We previously discussed the operations of image-charge QCA circuits. Producing a complete functional system requires setting polarization of the input cell (writing operation) and detecting the polarization of the output cell (reading operation) in an image-charge QCA. We consider that the writing operation can be accomplished by the following method. First, we design a four-dot input cell in which electron tunneling between the dots is forbidden. Electron tunneling between the input cell and the other cells is also forbidden. Next, we can set the polarization state of the input cell using a STM/AFM tip to inject one electron into each of two quantum dots positioned diagonally in the cell. Even if the STM/AFM tip is removed, the polarization state of the input cell will remain stable, because tunneling between the dots is forbidden in the input cell. Finally, we can switch the polarization of the input cell from state 1 (0) to state 0 (1) by first pulling one electron each out of dots 2 and 4 (1 and 3) and then injecting one electron each into dots 1 and 3 (2 and 4). Because tunneling between the input cell and the other cells is also forbidden, the writing operation can be carried out for different input cells, and does not change the number of electrons in other cells.

The reading operation can be performed by detecting the polarization state of the output cell using a single-electron transistor (SET) electrometer. We calculated the voltage potential near the output cell of the image-charge QCA circuits and discovered that the voltage potential distribution changes markedly when the polarization of the output cell is switched. Figure 10 shows typical contour plots of voltage potential distributions near the output cell in the five-cell linear array circuit shown in Fig. 2(a). If the polarization state of the output cell is 1, then the difference V_{AB} of the voltage potentials at measuring points A and B is -4.4 mV; if the polarization state is 0, then V_{AB} is 4.4 mV. The SET electrometer[7] and single-electron transistor scanning electrometer (SETSE)[10] have shown a remarkable ability to detect static electric fields and individual charges. If we use the electrometers to measure the differences of the voltage potential distribution, the polarization state of the output cell can be detected. Details of the operations will be investigated in the future.

Successful experiments on (1) electron injection into (extraction from) a quantum dot using a STM tip[11] and (2) measurement of the static electric field using a SET electrome-

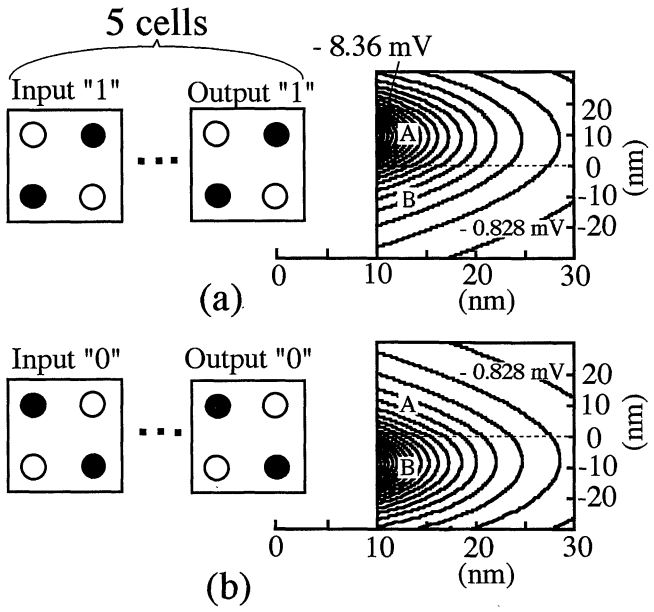

Fig. 10. Contour plots of voltage potential distribution near an output cell of the image-charge QCA linear array circuit: (a) when the state of the output cell is 1; (b) when the state of the output cell is 0. A and B show measuring points of a SET electrometer.

ter[10] have been carried out for other research objectives. We believe that these techniques can be applied to our image-charge QCA system.

6. Summary

We propose a novel device structure, an *image-charge QCA*. An image-charge QCA circuit is constructed on a metallic substrate covered with an insulator thin film. Its unit cell consists of four quantum dots. The barrier between the neighboring cells is designed to allow intercellular electron tunneling so that electrons can move among all the cells in the circuit. An image-charge QCA cell can overcome two basic problems: establishing charge neutrality in each cell as well as loading electrons easily and precisely. Image charges establish a cell's charge neutrality naturally and form dipoles with the excess electrons. The dipoles move among the cells of an image-charge circuit. We designed signal-transmission and elemental logic circuits using the image-charge QCA cells and analyzed their operation by means of the Monte Carlo simulation method. We demonstrated that the image-charge QCA can perform signal transmission as well as elemental logic operations and that electron loading can be easily performed by injecting electrons from one end cell into the circuit at a rate of two electrons per cell with a STM/AFM tip.

Acknowledgement

This work was supported by a Grand-in-Aid for Scientific Research (C#08650396) from the Ministry of Educations, Science, Sports and Culture.

1) C. S. Lent, P. D. Tougaw, W. Porod and G. H. Bernstein: Nanotechnology **4** (1993) 49.
2) C. S. Lent and P. D. Tougaw: J. Appl. Phys. **75** (1994) 4077.
3) T. Tanamoto, R. Katoh and Y. Naruse: Jpn. J. Appl. Phys. **33** (1994) L1502.
4) Y. Takahashi, A. Fujiwara, M. Nagase, H. Namatsu, K. Kurihara, K. Iwadate and K. Murase: IEICE Trans. Electron. **E79-C** (1996) 1503.
5) K. Matsumoto, M. Ishii, K. Segawa, Y. Oka, B. J. Vartanian and J. S. Harris: Appl. Phys. Lett. **68** (1996) 34.
6) M. Kato: Phys. Rev. B **51** (1995) 16046.
7) M. H. Devoret and H. Grabert, *Single Charge Tunnelling Coulomb Blockade Phenomena in Nanostructures* (Plenum Press New York, 1992).
8) N. Kuwamura, K. Taniguchi and C. Hamaguchi: Trans. IEICE **J77-C** (1994) 221.
9) N.-J. Wu, N. Asahi and Y. Amemiya; Jpn. J. Appl. Phys. **36** (1997) 2621.
10) M. J. Yoo, T. A. Fulton, H. F. Hess, R. L. Willett, L. N. Dunkleberger, R. J. Chichester, L. N. Pfeiffer and K. W. West: Science **276** (1997) 579.
11) R. Wilkins, E. Ben-Jacob and R. C. Jaklevic: Phys. Rev. Lett. **63** (1989) 801.